

# Functions from $\mathbb{R}^2$ to $\mathbb{R}^2$ : a study in nonlinearity

Nicolau C. Saldanha and Carlos Tomei

October 20, 2018

## 1 Introduction

Calculus students learn how to draw graphs of functions from  $\mathbb{R}$  to  $\mathbb{R}$  and undergraduates studying complex variable learn about geometric properties of functions like  $f(z) = z^3$  and  $g(z) = e^z$ . Some teachers go further and introduce a few examples of conformal mappings. A picture is worth a thousand words, but more can be said on their favor: they provide a good exercise in combining theoretical facts in a consistent fashion. Indeed, to obtain the graph of a real function, a student considers its derivatives, asymptotic behavior and some special points, among other features. Something similar happens in the study of conformal mappings.

In this text, we consider functions from  $\mathbb{R}^2$  to  $\mathbb{R}^2$  and along the way assemble a number of tools from undergraduate courses. We describe a graphical representation of such functions and, for functions which are visually too complicated, we still count preimages, in a manner reminiscent of Rouché's theorem. Why is it that such aspects of functions from the plane to the plane are not more familiar? A reason might be the following. Most of the information we compute about functions from the line to itself, or about holomorphic functions, concerns special points—typically critical points, where the derivative is zero. In the case of functions from the plane to the plane, we need to consider critical curves, where the Jacobian matrix is not invertible. Such curves are often impossible to describe in simple closed form.

Enter the computer: we should think of the study of a given function from the plane to the plane as a description of certain relevant objects, in a way that these objects become amenable to numerics. In this sense, the time is ripe for this new case study in nonlinear theory, in the same way that we feel more at ease nowadays with showing students how to evaluate roots of polynomials of degree 6, or eigenvalues of  $5 \times 5$  matrices.

The theory should operate on two levels: we should learn enough to get qualitative information about simple examples, and we should be able to derive numerical procedures to handle general cases. In particular, such procedures

should extend our knowledge of the preimages of a point, from mere counting to explicit computation.

In section 2 we present a representative function  $F_0$  which will be our favorite test case throughout the paper; in section 10 some additional examples are discussed. Some of the tools required for this project belong to the standard curriculum, others are just ahead. All of them are basic when dealing with non-linear problems. Thus, for example, in section 3, we describe the local behavior of a function at *folds* and *cusps*, special critical points in the domain where the inverse function theorem does not apply. We will compute winding numbers and will also consider, in section 8, the *rotation number* of a  $C^1$  curve. Some aspects of covering space theory, presented in sections 5 and 6, will help us fit together local information. In particular, we will be able to perform *compatibility checks*, discussed in section 9, which often indicate the presence of yet unknown critical curves.

Some theoretical aspects have computational counterparts. For example, under appropriate hypothesis, the inverse function theorem asserts that a function is locally invertible while Newton's method may be used to actually perform the inversion. More generally, the implicit function theorem verifies the regularity of critical curves and a predictor-corrector method then traces the curve, as in section 4. Similarly, covering space theory is closely related to numerical continuation methods, employed in section 7. Due to space limitations, we handle numerical aspects rather superficially, providing sketches of arguments and indicating more specific literature. Some results are quoted from standard references but we present proofs of a few statements which are harder to find in book form. Senior undergraduates should be able to follow through the arguments.

Together with Iaci Malta, the authors have published more technical texts ([13], [14]). The program (in rough form) which generated pictures and computations for this paper is available ([1]). Both theoretical and computational aspects can be extended to the study of functions from a bounded subset of the plane to the plane ([6]). For a more general study of the geometry of functions between two surfaces, see [7].

## 2 A first example

Our first and favorite example is the function

$$F_0 : \mathbb{R}^2 \rightarrow \mathbb{R}^2$$

$$\begin{pmatrix} x \\ y \end{pmatrix} \mapsto \begin{pmatrix} x^3 - 3xy^2 + 2.5x^2 - 2.5y^2 + x \\ 3x^2y - y^3 - 5xy + y \end{pmatrix}$$

which, in complex notation, can be written as  $F_0(z) = z^3 + 2.5\bar{z}^2 + z$ . Due to the presence of  $\bar{z}$ ,  $F_0$  is not holomorphic. As every Rouché fan would notice,  $F_0$  acts on concentric circles centered at the origin according to (at least) three different

regimes: figure 1 shows the images of circles with radii equal to 0.1, 1 and 10, respectively (the figures are not in scale).

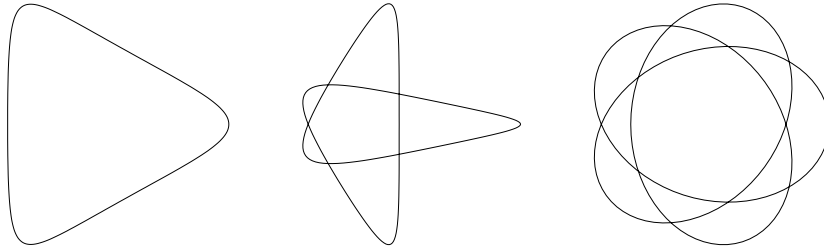


Figure 1: Three different regimes (radii 0.1, 1 and 10)

Indeed, orient the circles in the domain positively (i.e., counterclockwise). For radii close to 0,  $F_0$  takes these circles to simple closed curves with winding number 1 with respect to 0: this is clear from the fact that, close to the origin,  $F_0$  is essentially the identity. For radii close to 1, the term  $2.5\bar{z}^2$  dominates the other two ( $|2.5\bar{z}^2| > |z^3| + |z|$  for  $|z| \approx 1$ ) and one should expect the images of such circles to be closed curves winding twice around the origin with negative orientation—the winding number with respect to 0 of these curves is  $-2$ . Finally,  $F_0$  takes circles of large radius to curves winding three times positively around the origin:  $F_0$  near infinity looks like  $z^3$ .

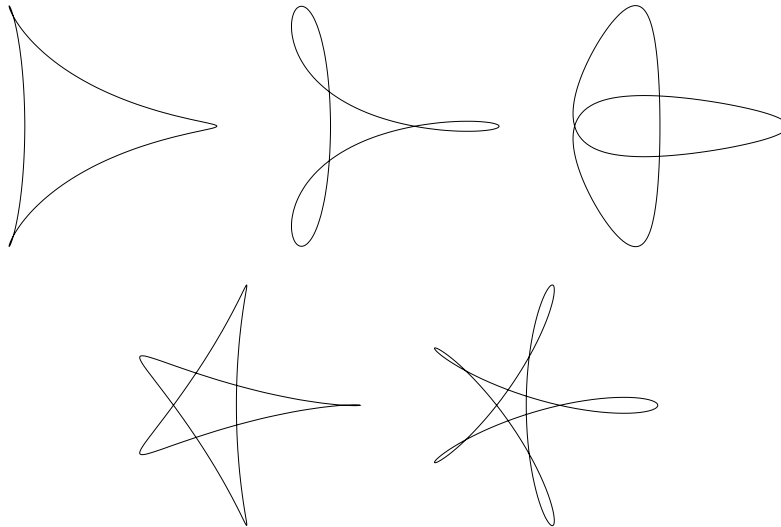


Figure 2: Interpolating regimes: radii 0.2, 0.3, 0.7, 1.5 and 2

How are the images of concentric circles changing from one regime to another? Figure 2 shows the images of intermediate circles of radii 0.2, 0.3, 0.7, 1.5 and

2. It may be hard to see in the picture, but there are two small loops in the first figure and one in the fourth; the five curves are indeed smooth. We will address the formation of these patterns in the sequel. We will draw other, more informative pictures and will infer, for example, that the equation  $F_0(z) = 0$  has nine solutions.

### 3 Local theory

We will use some basic facts of the local theory of functions in the plane, obtained by Whitney in 1955 ([23]). The subject developed considerably under the name of singularity theory after the work of Thom and Mather in the sixties. An excellent reference with emphasis in applications is [9]; a more technical one is [8].

Recall that, for a smooth function  $F : \mathbb{R}^2 \rightarrow \mathbb{R}^2$ , a point  $p$  is *regular* if the Jacobian  $DF(p)$  is an invertible matrix. From the inverse function theorem ([11], chap. XVII, §3, pg. 349), after smooth changes of variable in appropriate neighborhoods of a regular point  $p$  and its image  $F(p)$ , the function  $F$  takes the form  $\tilde{F}(x, y) = (x, y)$ ; more precisely, there exist local diffeomorphisms  $\Phi$  and  $\Psi$  with  $F = \Phi \circ \tilde{F} \circ \Psi$  as above. Points which are not regular are *critical* and they form the *critical set*  $C$ . A critical point  $p_f$  is a *fold point* (or, more informally, a fold) if, after changing variables near  $p_f$  and  $F(p_f)$ ,  $F$  becomes  $\tilde{F}(x, y) = (x, y^2)$ . Also, a critical point  $p_c$  is a *cuspid point* (or, again, simply a cusp) if changes of variables convert  $F$  into  $\tilde{F}(x, y) = (x, y^3 - xy)$ . The formulae for  $\tilde{F}$  are the *normal forms* of a function at a fold and at a cusp: they imply that in appropriate neighborhoods of folds and cusps, the critical set is a smooth arc consisting of folds and cusps; also, cusps are isolated.

In the same way that the hypothesis of the inverse function theorem guarantees a simple normal form of a function near a regular point, there are explicit conditions which characterize folds and cusps. For example, a critical point  $p_f$  is a fold of a smooth function  $F : \mathbb{R}^2 \rightarrow \mathbb{R}^2$  if two conditions hold. First, the gradient of  $\det DF$  should be nonzero at  $p_f$ , which implies, from the implicit function theorem, that the critical set near  $p_f$  is a curve. Second,  $\text{grad } \det DF(p_f)$  should not be orthogonal to  $\ker DF(p_f)$ . There is a similar, more complicated characterization of cusps, which we omit.

A function near a fold behaves in a simple way. All properties described below can be checked by referring to the normal form. In figure 3, a small arc of the critical set and its image under the function  $F$  are indicated with thick lines for both types of critical points. Points in the domain with the same image are indicated by the same label. The thinner lines on both sides of the critical curves are taken to thin lines as indicated. Near a fold  $p_f$ , the function  $F$  takes points to a single side of the image of the critical arc. Thus, a point  $w$  near  $F(p_f)$  has 0, 1 or 2 preimages near  $p_f$ , depending on its position with respect to the image of the critical arc. The image of a curve  $\gamma$  *transversal* to the critical

set at a fold point is generically a nonsingular curve  $F(\gamma)$  tangent to  $F(C)$  (two smooth arcs are transversal at an intersection point if their tangent vectors are linearly independent). The inverse image of a curve  $\delta$  transversal to  $F(C)$  is a curve tangent to  $\ker(DF)$  at  $C$ . Only one side of  $\delta$  actually has preimages (in the figure, the dotted part of  $\delta$  is not in the image of  $F$  near  $p_f$ ).

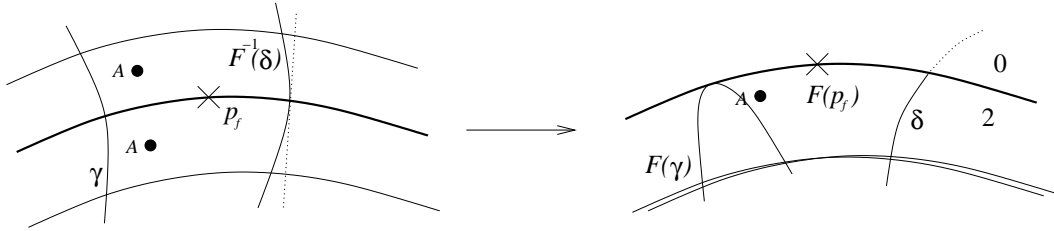


Figure 3: Local behavior near a fold

Points  $w$  near the image  $F(p_c)$  of a cusp  $p_c$  may have 1, 2 or 3 preimages near  $p_c$ . Arcs  $\gamma_1$  and  $\gamma_2$  in figure 4 have qualitatively different images:  $F(\gamma_1)$  undergoes a loop around  $F(p_c)$ ,  $F(\gamma_2)$  does not. We also indicate the (nontrivial) preimage of the image of the critical curve near the cusp: notice that it lies to one side of the critical curve. We say that the cusp is *effective* on that side.

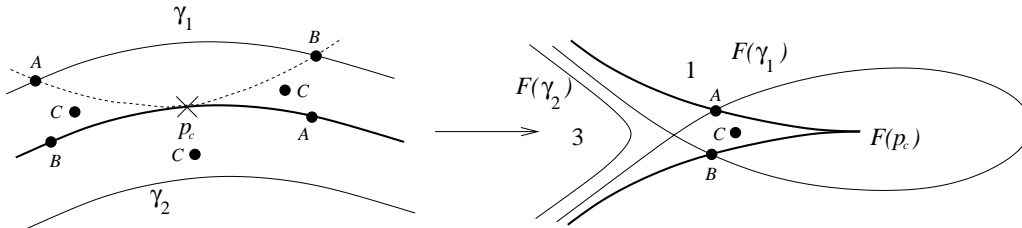


Figure 4: Local behavior near a cusp

Whitney defined *excellent functions* as functions having only folds and cusps as critical points. The regular points of an excellent function  $F : \mathbb{R}^2 \rightarrow \mathbb{R}^2$  form an open dense subset of the plane and its critical set  $C$  is a disjoint union of isolated smooth curves. It is easy to see from the normal form that cusps form a discrete set and the rest of  $C$  consists of arcs of folds. Fortunately, excellent functions from the plane to the plane are abundant: this allows us to ignore more complicated critical points.

**Theorem 1 (Whitney, [23])** *In the  $C^r$  topology on compact sets ( $r \geq 3$ ), the set of excellent functions  $F : \mathbb{R}^2 \rightarrow \mathbb{R}^2$  is residual.*

It is instructive to compare the local theory of excellent functions to the local theory of holomorphic functions: we remind the reader of the normal form of a holomorphic function at a critical point.

**Proposition 2** *Let  $f : A \rightarrow \mathbb{C}$  be a holomorphic function with a critical point  $z_0$  which is a zero of order  $n-1$  of  $f'$ . Then its normal form is given by  $\tilde{f}(w) = w^n$ . More precisely, there exist local holomorphic diffeomorphisms  $\phi, \psi$  with  $\phi(0) = f(z_0)$ ,  $\psi(z_0) = 0$  for which  $f = \phi \circ \tilde{f} \circ \psi$  in a neighborhood of  $z_0$ .*

The open mapping theorem and the maximum modulus theorem ([4], chapters 6 and 7) follow easily from this local form.

**Proof:** Write

$$f(z) = a + b(z - z_0)^n g(z) = a + b((z - z_0)h(z))^n, \quad a = f(z_0), \quad b = f^{(n)}(z_0)/n!,$$

where  $g$  and  $h$  are holomorphic functions with  $g(z_0) = h(z_0) = 1$  and  $g(z) = (h(z))^n$ . Now set  $\phi(u) = a + bu$ ,  $\psi(z) = (z - z_0)h(z)$  and we are done. ■

In particular, critical points of nonconstant holomorphic functions are isolated and they certainly may not be folds or cusps. How can Whitney's theorem be true then? An excellent function  $F$  near a holomorphic function  $f$  must be non-holomorphic. For instance, to approximate  $f(z) = z^7$  by an excellent function, one may try  $F(z) = z^7 + \epsilon \bar{z}$ , which indeed works for small  $\epsilon$ . There is a natural counterpart to Whitney's theorem for holomorphic functions: in a residual set of holomorphic functions, the second derivative is nonzero at all critical points.

## 4 Tracing the critical set

Searching for critical curves by hand is hard even for a polynomial map of low degree, such as our  $F_0$ . Classifying critical points as folds, cusps or yet something else is even harder. A more practical approach is to go through numerical computations. In order to study the critical set of a function  $F$ , our program first searches for points  $p_+$  and  $p_-$  for which  $DF(p_+)$  and  $DF(p_-)$  have determinants of opposite sign. By continuity, there must be a critical point  $p_0$  (i.e.,  $\det DF(p_0) = 0$ ) in the segment joining  $p_+$  and  $p_-$ . After computing  $p_0$ , the program obtains some points  $p_1, p_2, \dots$  in the critical curve through  $p_0$  (i.e., the level through  $p_0$  of  $\det DF_0$ ) by a *predictor-corrector method* (a fine presentation of this class of methods is given in [3]). A very simple example of this technique is the following. As in figure 5, draw a tangent line to the critical curve through  $p_0$  and take a point  $q$  on this line at a short distance  $h$  from  $p_0$ . Now through  $q$  draw a second line parallel to  $\text{grad } \det DF(q)$  and on this line solve  $\det DF(p_1) = 0$  by Newton's method with initial condition  $q$ .

As the critical points  $p_0, p_1, \dots$  are computed, the program checks the conditions characterizing folds for segments from  $p_i$  to  $p_{i+1}$ : this is done in order to

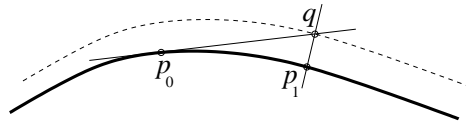


Figure 5: A simple predictor-corrector method

detect cusps (or other singularities). On segments which do not pass this test, the program searches for cusps and validates them with additional tests which we do not detail. These tests ascertain with considerable robustness and reliability that all critical points on this critical curve are indeed folds or cusps.

What is the critical set of  $F_0$ ? And for that matter, is it even excellent? The left part of figure 6 shows both critical curves  $\Gamma_1$  and  $\Gamma_2$  of the function  $F_0$ : they are ovals around the origin. The images of the critical curves are on the right:  $F_0(\Gamma_1)$  is a small curvilinear triangle surrounding the origin and  $F_0(\Gamma_2)$  is a stellated pentagon. Indeed, numerics confirm that the two critical curves have 3 and 5 cusps. This is in agreement with the almost polygonal shape of the images of circles of radii 0.2 and 1.6 in figure 2. The labels on the outer critical curve  $\Gamma_2$  are of two kinds: capital letters indicate cusps and lower case letters are preimages of self-intersections of  $F_0(\Gamma_2)$ . The three cusps on  $\Gamma_1$  are not indicated, but the reader may check that if  $\Gamma_1$  is traversed counterclockwise then so is  $F_0(\Gamma_1)$ .

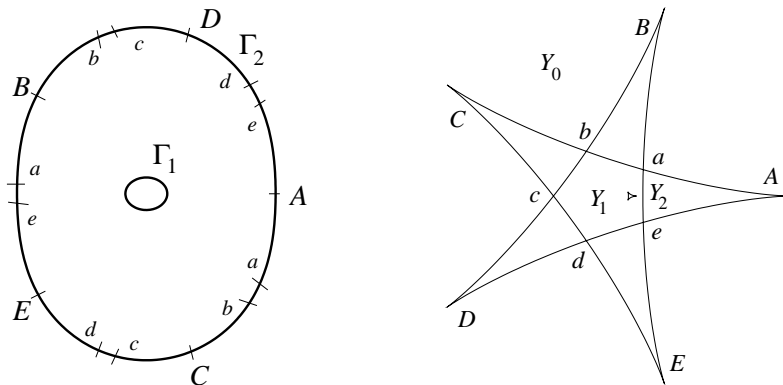


Figure 6: The critical curves of  $F_0$  and their images

Critical curves are thus described by lists of points, some of them cusps. Outside the known part of the critical set, however, very few points have been considered. Without a labor intensive search, how do we know if we have found all critical curves of a function? This, in general, is a nontrivial issue and we shall say more about it in section 9.

## 5 Counting preimages

We set the information obtained so far in a more robust setting lest the reader think that we are letting pictures take control over mathematical reasoning. We begin by stating without proof a stronger form of the Jordan curve theorem.

**Theorem 3** *Let  $\gamma \subset \mathbb{R}^2$  be a simple closed curve. The curve  $\gamma$  is the boundary of a closed topological disk  $D$ . The open set  $\mathbb{R}^2 - \gamma$  has precisely two connected components: the interior of  $D$  and the complement of  $D$ . Furthermore, if  $\gamma$  is a piecewise smooth curve then there exists a homeomorphism from  $D$  to the closed unit disk whose restriction to the interior of  $D$  is holomorphic.*

The first claim is known as the Schoenflies theorem for which a nice proof is given in [20]. The second is the standard Jordan theorem (theorem 13.4, chapter 8, [16]) and the third is an extension of the Riemann mapping theorem (14.19 in [19]).

We denote by  $D_\gamma$  the closed (topological) disk surrounded by the simple closed curve  $\gamma$  and by  $\text{int } D_\gamma$  the corresponding open disk. The lemmas that follow are standard, but somewhat hard to pinpoint in the literature.

**Lemma 4** *Let  $\gamma$  be a smooth simple closed curve in  $\mathbb{R}^2$ . Let  $F : D_\gamma \rightarrow \mathbb{R}^2$  be a  $C^0$  map which is  $C^1$  in  $\text{int } D_\gamma$ . Assume that  $F$  has no critical points in  $\text{int } D_\gamma$  and is injective on  $\gamma$ . Then  $F$  is a homeomorphism from  $D_\gamma$  to its image  $F(D)$ .*

**Proof:** For readers acquainted with degree theory, the proof is simpler; we sketch a more elementary argument. Set  $\delta = F(\gamma)$ : clearly,  $\delta$  is a simple, closed curve, surrounding a closed (topological) disk  $D_\delta$ . At every point  $p \in \text{int } D_\gamma$ ,  $F$  is open, i.e., a small open ball around  $p$  is taken bijectively to a small open set around  $F(p)$ : this follows from the inverse function theorem, since  $F$  has no critical points in  $\text{int } D_\gamma$ . Thus, any boundary point of  $F(D_\gamma)$  ought to be in  $F(\gamma) = \delta$ . By theorem 3, the compact set  $F(D_\gamma)$  equals either  $\delta$  or  $D_\delta$ ; on the other hand,  $F(D_\gamma) = \delta$  is impossible, since the interior of  $\delta$  is empty.

We now prove that  $F$  is injective: from the arguments above and the injectivity on  $\gamma$ , we only have to show that if  $p_0, p_1 \in \text{int } D_\gamma$  are such that  $F(p_0) = F(p_1)$  then  $p_0 = p_1$ . Let  $\zeta : [0, 1] \rightarrow \text{int } D_\gamma$  be a smooth path with  $\zeta(0) = p_0$ ,  $\zeta(1) = p_1$  so that  $(F \circ \zeta)(0) = (F \circ \zeta)(1)$ . Let  $H : [0, 1]^2 \rightarrow \text{int } D_\Gamma$  be a smooth function with  $H(0, t) = (F \circ \zeta)(t)$ ,  $H(s, 0) = H(s, 1) = H(1, t)$ : the existence of such  $H$  is ascertained by theorem 3. We now construct  $\zeta_s : [0, 1] \rightarrow \text{int } D_\gamma$  so that  $F(\zeta_s(t)) = H(s, t)$ :  $\zeta_s$  is the solution of the differential equation

$$\zeta_s(0) = p_0, \quad \zeta'_s(t) = (DF(\zeta_s(t)))^{-1} \frac{\partial H}{\partial t}(s, t).$$

Now  $\zeta_1$  is constant whence  $\zeta_1(1) = p_0$ . But  $\zeta_s(1)$  depends continuously on  $s$  and satisfies  $F(\zeta_s(1)) = F(p_0)$  for all  $s$ . Therefore  $\zeta_s(1) = p_0$  for all  $s$  and  $p_1 = \zeta_0(1) = p_0$ .

Since  $F$  is a continuous bijection from the compact set  $D_\gamma$  to the Hausdorff space  $D_\delta$ ,  $F$  is a homeomorphism (theorem 5.6, chapter 3, [16]). ■

A continuous function  $F : \mathbb{R}^2 \rightarrow \mathbb{R}^2$  is *proper* if the inverse of any compact set is compact. The reader should have no difficulty in proving that this is equivalent to saying that  $\lim_{p \rightarrow \infty} F(p) = \infty$ . Our function  $F_0$  is proper.

**Lemma 5** *Let  $F : \mathbb{R}^2 \rightarrow \mathbb{R}^2$  be a proper excellent function. The number of preimages under  $F$  of any point of  $\mathbb{R}^2$  is finite.*

**Proof:** By properness, all preimages of a point  $w$  belong to a closed disk  $D$ . If there are infinitely many of them, they must accumulate at a point  $p$ , which, by continuity of  $F$ , is also a preimage of  $w$ . Now,  $p$  may not be either regular, a fold or a cusp, since the three normal forms do not allow for infinitely many local preimages, in disagreement with the excellence of  $F$ . ■

Given a closed set  $X \subset \mathbb{R}^2$ , we call the connected components of  $\mathbb{R}^2 - X$  the *tiles for  $X$* .

**Lemma 6** *Let  $F : \mathbb{R}^2 \rightarrow \mathbb{R}^2$  be a proper excellent function with critical set  $C$ . On each tile  $A$  for  $F(C)$ , the number of preimages of  $F$  is a constant.*

**Proof:** By connectivity, it suffices to show that the number of preimages of points near  $w \in A$  is constant. Let  $p_1, \dots, p_k$  be the (finitely many) preimages of  $w$ . By hypothesis, they are regular points, and thus there are open disjoint neighborhoods  $V_i, i = 1, \dots, k$ , with  $p_i \in V_i$  and so that  $F$  restricts as a homeomorphism from each  $V_i$  to an open neighborhood  $W$  of  $w$ . Thus, points in  $W$  have at least as many preimages as  $w$ . Suppose now that for a sequence  $w_j \in W$  converging to  $w$ , the points  $w_j$  have more preimages than  $w$ . For each  $w_j$ , call one such preimage  $p_j^* \notin \cup_i V_i$ . By properness, the sequence  $\{p_j^*\}$  must accumulate to a point  $w_\infty$ , and, again by continuity,  $w_\infty$  must be a preimage of  $w$  which does not belong to the interior of  $\cup_i V_i$ : this gives rise to a new preimage of  $w$ , a contradiction. ■

A proper excellent function  $F : \mathbb{R}^2 \rightarrow \mathbb{R}^2$  is *nice* if the following two conditions hold:

- any point  $y$  in  $F(C)$  is the image of at most two critical points;
- if  $q$  is the image of two critical points  $p_1$  and  $p_2$  then both are folds and the tangent lines to  $F(C)$  at  $q$  corresponding to  $p_1$  and  $p_2$  are distinct.

Points which are images of two critical points are *double points*. Rather unsurprisingly, the generic excellent function is nice, but we do not prove this technical result. From figure 6, the function  $F_0$  is nice. Two distinct tiles  $A$  and  $B$  for  $F(C)$  are *adjacent* if their boundaries share an arc of  $F(C)$ . In figure 6, tiles  $Y_0$  and  $Y_1$  are both adjacent to  $Y_2$  but not to each other.

**Lemma 7** *Let  $F : \mathbb{R}^2 \rightarrow \mathbb{R}^2$  be a nice function with critical set  $C$ ; the number of preimages of points in adjacent tiles for  $F(C)$  differ by two.*

**Proof:** Take  $w$  to be the image of a fold  $p$  belonging to a common boundary arc of adjacent tiles  $A$  and  $B$ . Let  $p_1, \dots, p_k$  be the preimages of  $w$ , with  $p = p_1$ . As in the proof of the previous lemma, we take disjoint open neighborhoods  $V_i$  of  $p_2, \dots, p_k$  not containing  $p$  which are taken homeomorphically by  $F$  to an open neighborhood  $W$  of  $w$ . Take points  $w_A \in A \cap W$ ,  $w_B \in B \cap W$ : there will be  $k - 1$  preimages of  $w_A$  and  $w_B$  in the neighborhoods  $V_i$ . Now, from the behavior of  $F$  near  $p$ , either  $w_A$  or  $w_B$  has two additional preimages close to  $p$ . ■

How can we obtain the *sense of folding*, i.e., on which of the two adjacent tiles for  $F(C)$  do points have more preimages? One way is to look at images of cusps: from figure 4, points inside the wedge have more preimages than points outside it.

## 6 Covering maps and the flower

We now split the domain of a nice function  $F$  in regions on which  $F$  behaves in a very simple fashion. More precisely, we consider the tiles for  $F^{-1}(F(C))$ , the *flower* of  $F$ . Figure 7 shows the flower of  $F_0$ .

The two critical curves  $\Gamma_1$  and  $\Gamma_2$  are of course part of the flower and are drawn thicker. The labels indicate preimages of special points in the image, given in figure 6. The local behavior at the eight cusps of  $F_0$  is in agreement with figure 4. Cusps in  $\Gamma_1$  are effective in the annulus between critical curves and cusps in  $\Gamma_2$  are effective in the region outside  $\Gamma_2$ . Notice the five small preimages of  $F_0(\Gamma_1)$  in the five petal-like tiles for the flower: these are indeed curvilinear triangles, as a zoom would show (one is shown in figure 10).

The tiles for the flower (resp. for  $F(C)$ ) will be labelled  $X_i$  (resp.  $Y_j$ ). As we shall see, for many  $X_i$ ,  $F$  is a diffeomorphism from  $X_i$  to some  $Y_j$ , extending to a homeomorphism between the closures  $\overline{X_i}$  and  $\overline{Y_j}$ . For the function  $F_0$ , for example, the only exceptions are  $X_0$  and  $X_1$ , indicated in figure 7. It turns out that each point of  $Y_0$  (see figure 6) has 3 preimages, all of them in  $X_0$ : this is in agreement with lemma 6 and the fact that  $F_0$  at infinity looks like  $z \mapsto z^3$ . Furthermore, points in the boundary of  $Y_0$  also have 3 preimages in the boundary of  $X_0$  but may have other preimages elsewhere: this can be checked by reading the labels in figures 6 and 7. Similarly, points in  $\overline{Y_1}$  have 2 preimages in  $\overline{X_1}$ . Still, the restrictions  $F : X_i \rightarrow Y_i$ ,  $i = 0, 1$ , are examples of *covering maps*, a concept whose basic properties we now review ([15] and [16] are excellent references).

Take  $X$  and  $Y$  to be open nonempty, connected subsets of  $\mathbb{R}^2$ : in our examples,  $X$  and  $Y$  will be tiles  $X_i$  and  $Y_j$ . The continuous function  $\Pi : X \rightarrow Y$  is a *covering map* if, for any  $y \in Y$ , there exists an open neighborhood  $V \subset \mathbb{R}^2$  of  $y$ , such that

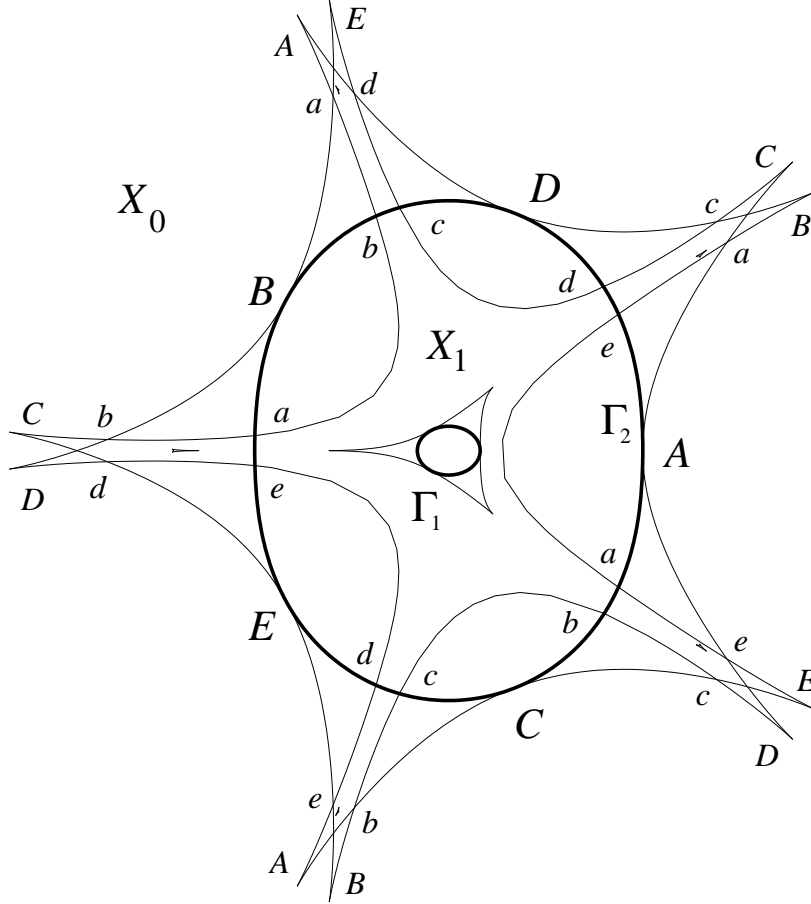


Figure 7: The flower  $F_0^{-1}(F_0(C))$

$V \cap Y$  is connected and, for any connected component  $Z$  of  $\Pi^{-1}(V \cap Y)$ , the restriction  $\Pi : Z \rightarrow V \cap Y$  is a homeomorphism.

**Proposition 8** *Let  $F : \mathbb{R}^2 \rightarrow \mathbb{R}^2$  be a nice function with critical set  $C$ . Let  $X_i$  and  $Y_j$  be the tiles for the flower  $F^{-1}(F(C))$  and  $F(C)$ . Then the image of each tile  $X_i$  is a tile  $Y_j$ , the restriction  $F : X_i \rightarrow Y_j$  is a covering map and  $F : \overline{X_i} \rightarrow \overline{Y_j}$  is locally injective.*

It is not always true that  $F : \overline{X_i} \rightarrow \overline{Y_j}$  is injective: the boundary may contain two regular preimages of a double point.

**Proof:** Since  $F(X_i) \subseteq \mathbb{R}^2 - F(C)$  is connected, it is contained in a single  $Y_j$ . Our proof of lemma 6 shows that the number  $k$  of preimages under  $F$  in  $X_i$  is the same for any point  $y \in Y_j$  (and therefore  $k > 0$ ). The remaining argument is standard: given  $y \in Y_j$ , let  $x_1, \dots, x_k \in X_i$  be its preimages (lemma 5). These are all regular points: by the inverse function theorem there are disjoint open neighborhoods

$U_1, \dots, U_k \subset X_i$  of  $x_1, \dots, x_k$  taken diffeomorphically to  $V_1, \dots, V_k$ . Take  $V$  to be a small ball centered on  $y$  contained in  $V_1 \cap \dots \cap V_k$ . This is the neighborhood of  $y$  requested in the definition of covering map. Indeed, since the number of preimages is constant, there are no other preimages of  $V$  outside  $U_1 \cup \dots \cup U_k$ . ■

From the behavior of  $F_0$  near infinity, elements of large absolute value in the image of  $F_0$  have exactly three preimages. Now, by lemmas 6 and 7 (using cusps to determine the sense of folding, as suggested at the end of section 5), we learn that the number of preimages in the tiles for  $F_0(C)$  vary as indicated in the left part of figure 8. The origin, which is at the very center of the innermost tile, has 9 preimages. We can actually compute these preimages, as we shall discuss in the next section: they are the three conjugate pairs  $1.864148 \pm 1.450656 i$ ,  $-0.818866 \pm 2.665700 i$ ,  $0.204718 \pm 0.319589 i$  and the three real numbers 0,  $-0.5$  and  $-2$ .

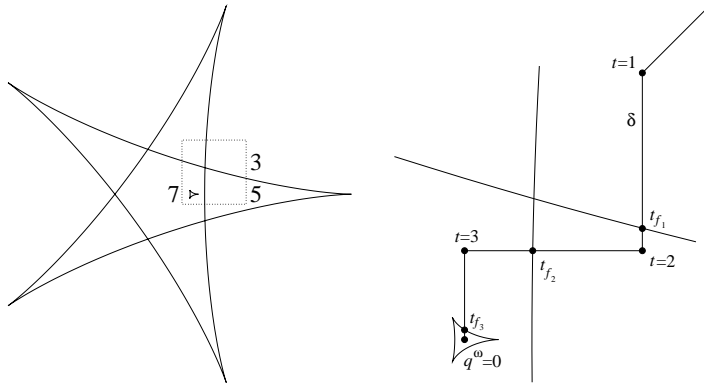


Figure 8: Counting and computing preimages

We shall make use of the so called universal cover of an open subset of the plane, as in following classical result.

**Theorem 9** *Let  $X \subset \mathbb{R}^2$  be a nonempty connected open set; then there exists a covering map  $\Pi : \mathbb{R}^2 \rightarrow X$ .*

A sketch of proof could be as follows. Consider  $X \subset \mathbb{C}$ : if  $X = \mathbb{C}$  or  $X = \mathbb{C} - \{z_0\}$  set  $\Pi(z) = z$  or  $\Pi(z) = z_0 + \exp(z)$ . Otherwise, take  $z_0 \in X$  and let  $\Delta = \{z \in \mathbb{C} \mid |z| < 1\}$ : clearly,  $\Delta$  and  $\mathbb{R}^2$  are diffeomorphic. Let  $\mathcal{F}$  be the (nonempty) class of holomorphic functions  $f : \Delta \rightarrow X$ ,  $f(0) = z_0$ ,  $f'(0) > 0$ . In  $\mathcal{F}$ , there exists a function  $f_0$  with maximum derivative at the origin. Existence, uniqueness and the fact that  $f_0 \circ \Pi$  is a covering map follow as in the proof of the Riemann mapping theorem in [2] or [19]. With this proof, the theorem above is a special case of the uniformization theorem (sections 3.2 and 3.3 of [12]).

## 7 Computing preimages

To compute preimages we use *continuation methods*, an example of which we now describe (see [3] for more). Let  $F : \mathbb{R}^2 \rightarrow \mathbb{R}^2$  be a nice function with critical set  $C$ , and take  $p^\alpha$  to be a regular point with image  $q^\alpha = F(p^\alpha)$ . For a point  $q$  sufficiently close to  $q^\alpha$ , Newton's method computes the only preimage  $p$  of  $q$  near  $p^\alpha$  by solving  $F(p) = q$ , taking  $p^\alpha$  as the initial iteration. Suppose now that we want to compute a preimage of a point  $q^\omega$  which is rather far from  $q^\alpha$ . We draw a smooth parametrized arc  $\delta : [0, 1] \rightarrow \mathbb{R}^2$  with  $\delta(0) = q^\alpha$ ,  $\delta(1) = q^\omega$  and try to obtain points along a continuous path  $\gamma : [0, 1] \rightarrow \mathbb{R}^2$  with  $\gamma(0) = p^\alpha$ ,  $F(\gamma(t)) = \delta(t)$ . More precisely, set  $t_0 = 0 < t_1 < t_2 < \dots < t_N = 1$  and try to compute  $\gamma(t_{i+1})$  by solving  $F(\gamma(t_{i+1})) = \delta(t_{i+1})$  taking  $\gamma(t_i)$  as initial condition for Newton's method. If  $\delta$  does not intersect  $F(C)$  and the distances  $t_{i+1} - t_i$  are taken to be sufficiently small then the method is guaranteed to obtain  $p^\omega = \gamma(1)$ , a preimage of  $q^\omega$ . This follows from the properness of  $F$  combined with the Newton-Kantorovich theorem (theorem 12.6.2, page 421, [17]). If  $\delta$  crosses  $F(C)$ , this continuation method may fail. For instance, if  $\delta(t_f) = F(p_f)$ , where  $p_f$  is a fold point, as in figure 3,  $\delta(t)$  belongs to the solid part of  $\delta$  for  $t < t_f$  (i.e.,  $\delta(t)$  belongs to the tile for  $F(C)$  adjacent to  $F(p_f)$  with the larger number of preimages) and  $\gamma(t)$  approaches  $p_f$  when  $t$  tends to  $t_f$  then any continuation method ought to fail: the dotted part of  $\delta$  has no preimage near  $p_f$  and no continuous function  $\gamma$  with the required properties exists.

We now consider the problem of computing all preimages of a point  $q^\omega \notin F(C)$ . Assume that there exists  $q^\alpha \notin F(C)$  for which all preimages  $p_1^\alpha, \dots, p_n^\alpha$  are known. Draw a piecewise smooth arc  $\delta$  from  $q^\alpha$  to  $q^\omega$  which crosses  $F(C)$  transversally at simple images of folds: our strategy is to start with the set of all preimages of  $q^\alpha$  and obtain all preimages of  $q^\omega$  by an extension of a standard continuation method along  $\delta$ . We may assume by induction that  $\delta$  is smooth and intersects  $F(C)$  exactly once at  $\delta(t_f) = q_f$ . Continuation along  $\delta$  starting at each  $p_i^\alpha$  tries to obtain paths  $\gamma_i$  with  $\gamma_i(0) = p_i^\alpha$ ,  $F(\gamma_i(t)) = \delta(t)$ . As we saw above, if  $\delta$  crosses  $F(C)$  from a tile with more preimages to a tile with fewer preimages then two of the paths  $\gamma_i$  will collide at  $p_f$  and will not be defined for  $t > t_f$ : that is not a problem for us since the remaining paths will still provide us with all the  $n - 2$  preimages of  $q^\omega$ . This scenario is reversed if  $\delta$  crosses  $F(C)$  from a tile with fewer preimages (dotted in figure 3) to a tile with more preimages: two new arcs are born at  $p_f$ . More precisely, two distinct paths  $\gamma_{n+1}$  and  $\gamma_{n+2}$  from  $[t_f, 1]$  to  $\mathbb{R}^2$  exist with  $\gamma_i(t_f) = p_f$  and  $F(\gamma_i(t)) = \delta(t)$  for  $i = n + 1, n + 2$ ,  $t \geq t_f$ . These paths are quite removed from any of the  $n$  preimages  $\gamma_i(t_f - \epsilon)$ ,  $i = 1, \dots, n$ , of  $\delta(t_f - \epsilon)$  (for a small  $\epsilon > 0$ ) and could not possibly be obtained from these by a (local) continuation method. Also, since the Jacobian  $DF(p_f)$  is not invertible,  $p_f$  (which we know, since we previously obtained the critical curves) is not acceptable as an initial condition for Newton's method to solve  $F(p) = q$  in  $p$ . Instead, we compute a unit generator  $v$  for  $\ker DF(p_f)$  and set

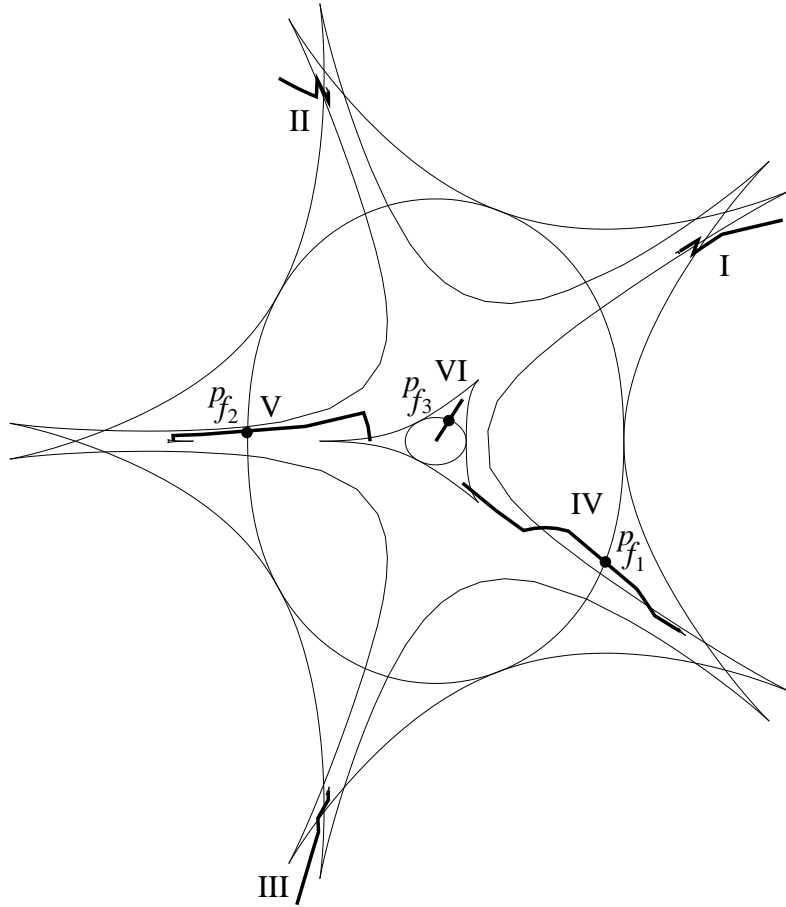


Figure 9: Inverting a path

$p_{n+1} = p_f + sv$ ,  $p_{n+2} = p_f - sv$  (for a small positive real number  $s$ ) and  $q_i = F(p_i)$  ( $i = n+1, n+2$ ). From the normal form, each  $q_i$  is now not too far from  $\delta(t_f + \epsilon)$  (for some small  $\epsilon$ ) and can be connected to it by an auxiliary arc  $\delta_i$  which does not intersect  $F(C)$ : our continuation method now obtains  $\gamma_i(t_f + \epsilon)$  by following  $\delta_i$ , starting with  $p_i$ . Recall that the preimage of any smooth curve  $\delta$  crossing  $F(C)$  transversally at  $q_f$  is tangent to  $v$  at  $p_f$  (figure 3).

Let us now go back to our basic example and see how our program obtains the nine preimages of 0 under  $F_0$ . First it computes the critical set  $C$  of  $F_0$  and its image, presented in figure 6. Next, it obtains the three preimages of a remote point  $q^\alpha$  (see figure 8). This is rather simple: for complex numbers  $z$  of large absolute value the function  $F_0(z)$  is similar to  $z \mapsto z^3$  and the three complex cube roots of  $q^\alpha$  are good initial conditions for a Newton-like method to solve  $F_0(p_i^\alpha) = q^\alpha$ ,  $i = 1, 2, 3$ . The three preimages lie in the regions indicated by the Roman numerals I, II and III in figure 9.

A path  $\delta : [0, 4] \rightarrow \mathbb{R}^2$  from  $q^\alpha = \delta(0)$  to  $0 = \delta(4)$  (as in figure 8) was constructed as a juxtaposition of four smooth paths defined on intervals with integer endpoints. The first ( $0 \leq t \leq 1$ ) is the only one that does not cross  $F_0(C)$ . Notice that the number of preimages is increasing along this path.

Three paths  $\gamma_i : [0, 4] \rightarrow \mathbb{R}^2$ ,  $i = 1, 2, 3$ , were obtained by a continuation method starting from  $\gamma_i(0) = p_i^\alpha$ . The path  $\gamma_1$ , which is in region I, is presented in figure 10;  $\gamma_2$  and  $\gamma_3$  are in regions II and III in figure 9. The whole inversion procedure from  $\gamma_i(0)$  to  $\gamma_i(4)$  does not cross a critical curve of  $F_0$ , and three solutions to the equation  $F_0(z) = 0$  are obtained:  $\gamma_1(4) \approx (1.864148, 1.450656)$ ,  $\gamma_2(4) \approx (-0.818866, 2.665700)$  and  $\gamma_3(4) \approx (-0.818866, -2.665700)$ .

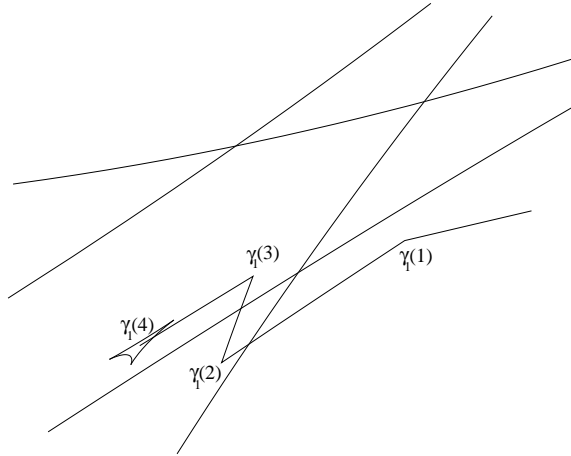


Figure 10: Zoom on region I of figure 8

The paths obtained by continuation within regions I, II and III do not notice anything unusual at  $t_{f_1}$ , the first intersection between  $\delta$  and  $F_0(C)$ . As we saw, however, two new arcs  $\gamma_4$  and  $\gamma_5$  are born at the critical point  $p_{f_1}$  for which  $F_0(p) = \delta(t_{f_1})$ . The program identified  $p_{f_1} = \gamma_4(t_{f_1}) = \gamma_5(t_{f_1})$ , which turns out to lie in the outer critical curve, and obtained by continuation from  $p_{f_1}$  two new paths, lying in region IV. Similarly, two new paths are born at  $t_{f_2}$  from the fold  $p_{f_2}$  (they are in region V) and yet two more at  $t_{f_3}$  from  $p_{f_3}$  (in region VI).

These computations rely heavily on the assumption that the critical set of  $F_0$  has been correctly identified. This is the same issue raised at the end of section 4; we next introduce topological tools to tackle this problem.

## 8 Rotation numbers

We remind the reader of a few facts concerning winding numbers (for a more complete exposition, see [5], sections 17 to 27). For a continuous function  $\phi :$

$[a, b] \rightarrow \mathbb{R}^2$  and  $p \in \mathbb{R}^2$ ,  $p$  not in the image of  $\phi$ , define a continuous *argument function*  $\theta_p : [a, b] \rightarrow \mathbb{R}$  such that

$$\phi(t) = |\phi(t) - p|(\cos \theta_p(t), \sin \theta_p(t))$$

for all  $t \in [a, b]$ . The argument function is unique up to an additive constant of the form  $2\pi n$  and the *angle swept* by  $\phi$  with respect to  $p$ ,  $A_p(\phi, p) = \theta_p(b) - \theta_p(a)$ , is well defined. Parametrize the standard unit circle by  $e : [0, 2\pi] \rightarrow \mathbb{S}^1$ , where  $e(t) = (\cos t, \sin t)$ . For a closed curve  $c : \mathbb{S}^1 \rightarrow \mathbb{R}^2$  with  $p$  not in the image of  $c$  we have that  $W(c, p) = A_p(c \circ e, p)/(2\pi)$  is an integer which we call the *winding number* of  $c$  around  $p$ .

A *homotopy* between continuous functions  $\phi_0 : [a, b] \rightarrow \mathbb{R}^2$  and  $\phi_1 : [a, b] \rightarrow \mathbb{R}^2$  is a continuous function  $\Phi : [0, 1] \times [a, b] \rightarrow \mathbb{R}^2$  with  $\Phi(0, t) = \phi_0(t)$  and  $\Phi(1, t) = \phi_1(t)$ . The winding number around  $p$  is invariant under homotopy provided all curves are closed and avoid the point  $p$ . More precisely, let  $\Phi : [0, 1] \times [a, b] \rightarrow \mathbb{R}^2$  be a homotopy between  $\phi_0 : [a, b] \rightarrow \mathbb{R}^2$  and  $\phi_1 : [a, b] \rightarrow \mathbb{R}^2$ , so that  $\Phi(s, a) = \Phi(s, b)$  for all  $s$ , for which  $p$  is not in the image of  $\Phi$ . Then we must have  $W(\phi_0, p) = W(\phi_1, p)$  (theorem 25.1 in [5]).

Of special interest will be *rotation numbers*: we present the basic results following [10] and [22]. A *parametrized regular closed curve* (in short, *prc-curve*) is a  $C^1$  function  $c : \mathbb{S}^1 \rightarrow \mathbb{R}^2$  with  $(c \circ e)'(t) \neq 0$  for all  $t \in [0, 2\pi]$ : the image of  $c$  is an oriented curve  $\gamma$ , possibly with self-intersections. The *rotation number*  $r(c)$  is the winding number of  $c'$  around 0:  $r(c) = W(c', 0)$ .

Two prc-curves  $c_0$  and  $c_1$  are *equivalent* if their images as oriented curves are equal, or, more precisely, if there exists an orientation preserving  $C^1$  diffeomorphism  $\eta : \mathbb{S}^1 \rightarrow \mathbb{S}^1$  with  $c_0 = c_1 \circ \eta$ . Equivalent curves have the same rotation number ([22]): this allows the computation of the rotation number of a prc-curve from the drawing of its image.

A recipe to compute  $r(c) = r(\gamma)$  is the following. Draw all horizontal and vertical tangent vectors to the oriented curve  $\gamma$  as in figure 11, measure the oriented angles between neighboring vectors (always equal to 0,  $\pi/2$  or  $-\pi/2$ ) add them all up and divide by  $2\pi$ . In the figure,  $r(\gamma) = 1$ . As another example, denote by  $e_\rho$  a counterclockwise parametrization of the circle of radius  $\rho$  around the origin. The curves in figure 1 are thus parametrized by  $F_0 \circ e_\rho$  for various values of  $\rho$ . Their rotation numbers are 1,  $-2$  and 3, respectively.

The following result, known as the *Umlaufsatz*, is somewhat harder to prove.

**Theorem 10 (Hopf, [10])** *If  $c$  is an injective prc-curve then  $r(c) = \pm 1$ .*

**Proof:** Let  $t_0 \in \mathbb{S}^1$  be a point maximizing  $|c(t)|$ ,  $t \in \mathbb{S}^1$ . Let  $\ell$  be the line tangent to  $\gamma$ , the image of  $c$ , through  $c(t_0)$ . By construction,  $c(t_0)$  is the only common point between  $\ell$  and  $\gamma$  and  $\gamma$  is a subset of the half-plane defined by  $\ell$  containing the origin. Without loss, set  $t_0 = 0$ ,  $\ell$  to be the horizontal line  $y = -1$

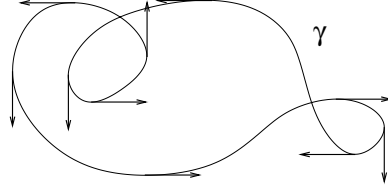


Figure 11: Computing rotation numbers

and  $(c \circ e)'(0) = (p, 0)$  where  $p > 0$ : in this case, we show that  $r(c) = 1$ . Let  $T = \{(s, t); 0 \leq s \leq t \leq 2\pi\}$  and  $\psi : T \rightarrow \mathbb{R}^2$  be defined by

$$\psi(s, t) = \begin{cases} (c \circ e)'(t) & \text{for } s = t, \\ -(c \circ e)'(0) & \text{for } s = 2\pi \text{ and } t = 0, \\ \frac{(c \circ e)(t) - (c \circ e)(s)}{\min\{t - s, 1 + s - t\}} & \text{otherwise.} \end{cases}$$

Since  $c$  is a  $C^1$  function,  $\psi$  is continuous; injectivity of  $c$  implies that  $\psi$  is never zero. The path  $\phi_1(t) = \psi(0, t)$ ,  $t \in [0, 2\pi]$ , satisfies  $\phi_1(0) = (p, 0)$ ,  $\phi_1(2\pi) = (-p, 0)$  and  $\phi_1(t)$  stays above the horizontal axis, whence  $\phi_1$  sweeps half a turn:  $A(\phi_1, 0) = \pi$ . Similarly, for  $\phi_2(s) = \psi(s, 2\pi)$ ,  $s \in [0, 2\pi]$ , we have  $A(\phi_2, 0) = \pi$ . Juxtapose  $\phi_1$  and  $\phi_2$  to define  $\phi_{12} : [0, 2\pi] \rightarrow \mathbb{R}^2$  where  $\phi_{12}(t) = \phi_1(2t)$  for  $t \in [0, \pi]$  and  $\phi_{12}(t) = \phi_2(2t - 2\pi)$  for  $t \in [\pi, 2\pi]$ : clearly,  $A(\phi_{12}, 0) = 2\pi$ . The function  $\psi$  can be viewed as a homotopy between  $(c \circ e)'$  (the restriction of  $\psi$  to  $\{(t, t), t \in [0, 2\pi]\}$ ) and  $\phi_{12}$  (the restriction to  $\{(0, t), t \in [0, 2\pi]\} \cup \{(s, 2\pi), s \in [0, 2\pi]\}$ ), showing that  $A((c \circ e)', 0) = A(\phi_{12}, 0) = 2\pi$  and thus  $r(c) = 1$ . ■

Two pre-curves  $c_0$  and  $c_1$  can be *deformed* into each other if there exists a continuous function  $H : [0, 1] \times [0, 2\pi] \rightarrow \mathbb{R}^2$  such that  $H(s, t) = c_s(e(t))$  for all  $s \in [0, 1]$ ,  $t \in [0, 2\pi]$ ,  $\frac{\partial H}{\partial t}$  is continuous and nonzero in  $[0, 1] \times [0, 2\pi]$  and  $\frac{\partial H}{\partial t}(s, 0) = \frac{\partial H}{\partial t}(s, 2\pi)$  for all  $s \in [0, 1]$ . As the next theorem shows, this is the appropriate concept of deformation on pre-curves, if we want to preserve rotation number. For instance, the curves in figure 1 do not admit deformations joining them.

**Theorem 11 (Graustein and Whitney, [22])** *Two pre-curves  $c_0$  and  $c_1$  can be deformed into each other if and only if  $r(c_0) = r(c_1)$ .*

**Proof:** The invariance of rotation number under deformation is a corollary of the invariance of winding number under homotopy: this proves one implication.

Now, let  $c_0$  and  $c_1$  be pre-curves with  $r(c_0) = r(c_1) = n$ . Reparametrize by arc length and change scale so that  $|(c_i \circ e)'(t)| = 1$  for all  $t \in [0, 2\pi]$ ,  $i = 0, 1$ . Let  $X : [0, 1] \times [0, 2\pi] \rightarrow \mathbb{S}^1 \subset \mathbb{R}^2$  be a continuous function with  $X(i, t) =$

$(c_i \circ e)'(t)$ ,  $X(s, 0) = X(s, 2\pi)$  and such that, for any  $s \in [0, 1]$ , the function  $t \mapsto X(s, t)$  is not constant: the existence of such  $X$  is a standard topological fact, but for completeness we provide an explicit construction. Let  $\theta_i : [0, 2\pi] \rightarrow \mathbb{R}$  be argument functions for  $(c_i \circ e)'$ : we have  $\theta_i(2\pi) - \theta_i(0) = 2\pi n$  for both values of  $i$ . For  $s \in [0, 1]$ , consider the segment joining  $\theta_0$  and  $\theta_1$ :  $\tilde{\theta}_s(t) = (1-s)\theta_0(t) + s\theta_1(t)$ . If  $n \neq 0$ ,  $\tilde{\theta}_s$  is clearly not a constant function and we take  $X(s, t) = e(\tilde{\theta}_s(t))$ . For  $n = 0$ , take  $\theta_{1/2} : [0, 2\pi] \rightarrow \mathbb{R}$  to be an arbitrary continuous function with  $\theta_{1/2}(0) = \theta_{1/2}(2\pi)$  which is not contained in the linear subspace generated by  $\theta_0$ ,  $\theta_1$  and the constant function 1. Define  $\theta_s$ ,  $s \in [0, 1]$ , by juxtaposing segments from  $\theta_0$  to  $\theta_{1/2}$  and from there to  $\theta_1$ ; take  $X(s, t) = e(\theta_s(t))$ . Let

$$m(s) = \frac{1}{2\pi} \int_0^{2\pi} X(s, t) dt \quad \text{and} \quad Y(s, t) = X(s, t) - m(s).$$

Notice that  $|m(s)| < 1$  and therefore  $Y(s, t) \neq 0$  for all  $s$  and  $t$ . Also, for any given  $s$ , the integral of  $Y(s, t)$  is 0 so that  $c_s$  defined by

$$(c_s \circ e)(t) = \int_0^t Y(s, \tau) d\tau$$

is a pre-curve. This is the required deformation. ■

Two different parametrizations of the same oriented smooth curve  $\gamma$ , yielding two pre-curves, have the same rotation and can therefore be deformed into each other. We may therefore ask, without ambiguity, whether two smooth curves  $\gamma_0$  and  $\gamma_1$  can be deformed into each other (within the class of pre-curves  $c_s : \mathbb{S}^1 \rightarrow \mathbb{R}^2$ ): this happens if and only if  $r(\gamma_0) = r(\gamma_1)$ .

## 9 Compatibility checks

Suppose that we have detected some critical curves, forming a certain subset  $C_1$  of the critical set  $C$  of an excellent function  $F$ . The propositions in this section provide global compatibility checks on  $C_1$ , i.e., necessary (but not sufficient) conditions for  $C_1 = C$ . We start with a technical lemma.

**Lemma 12** *Let  $U \subseteq \mathbb{R}^2$  be a connected open set and let  $\gamma_0, \gamma_1$  be positively oriented smooth simple closed curves bounding closed topological disks  $\Delta_0, \Delta_1 \subset U$ . Then  $\gamma_0$  can be deformed to  $\gamma_1$  within  $U$ , i.e., the image of the deformation is contained in  $U$ .*

**Proof:** Let  $\Pi : \mathbb{R}^2 \rightarrow U$  be a covering map (theorem 9) and consider  $\Pi^{-1}(\Delta_0)$ . This set is a disjoint union of closed disks: let  $\tilde{\Delta}_0$  be one of them and  $\tilde{\gamma}_0$  its boundary. Construct  $\tilde{\gamma}_1$  similarly. Since  $\tilde{\gamma}_s$ ,  $s = 0, 1$ , are both simple curves,  $r(\tilde{\gamma}_0) = r(\tilde{\gamma}_1) = 1$  (theorem 10) and therefore  $\tilde{\gamma}_0$  may be deformed to  $\tilde{\gamma}_1$  (theorem 11). Composing this deformation with  $\Pi$  yields a deformation from  $\gamma_0$  to  $\gamma_1$  contained in  $U$ , as desired. ■

**Proposition 13** *Let  $F : \mathbb{R}^2 \rightarrow \mathbb{R}^2$  be an excellent smooth function with critical set  $C$ . Let  $\gamma$  be a positively oriented smooth simple closed curve bounding a closed topological disk  $\Delta$  with  $\Delta \cap C = \emptyset$ . Then  $F(\gamma)$ , the image of  $\gamma$  under  $F$ , is a smooth curve and  $r(F(\gamma)) = \text{sgn det } DF(p)$  for any  $p \in \Delta$ .*

Here  $\text{sgn}(x)$  is the usual sign function,  $\text{sgn}(x) = 1$  (resp.  $-1$ ) for  $x > 0$  (resp.  $x < 0$ ).

**Proof:** First notice that the result holds if  $F$  is affine and the curve  $\gamma$  is a circle:  $F(\gamma)$  is an ellipse and its orientation is given by  $\text{sgn det } DF(p)$ . Next consider an arbitrary  $F$  and  $p \notin C$ . The affine map  $\tilde{F}(v) = F(p) + DF(p) \cdot (v - p)$  is a  $C^1$  approximation of  $F$  around  $p$ : thus there exists  $\rho_0$  such that, if  $\gamma$  is a positively oriented circle of radius  $\rho$  around  $p$ ,  $0 < \rho < \rho_0$ , then  $|r(F(\gamma)) - r(\tilde{F}(\gamma))| < 1$  (the arguments of the tangent vectors are arbitrarily close for small  $\rho_0$ ). Since rotation numbers are integers,  $r(F(\gamma)) = r(\tilde{F}(\gamma))$ . Let now  $\gamma_0$  be arbitrary and  $\gamma_1$  be a small round circle around some  $p \in \Delta$ : use lemma 12 to deform  $\gamma_0$  to  $\gamma_1$  within the connected component of  $\mathbb{R}^2 - C$  containing  $p$ . Compose this deformation with  $F$  to conclude that  $r(F(\gamma_0)) = r(F(\gamma_1))$ . ■

**Proposition 14** *Let  $F : \mathbb{R}^2 \rightarrow \mathbb{R}^2$  be an excellent smooth function with critical set  $C$ . Let  $\gamma_0, \gamma_1, \dots, \gamma_n$  be positively oriented smooth simple closed curves bounding  $\Delta_n$ , a closed topological disk with  $n$  holes with  $\Delta_n \cap C = \emptyset$ . Assume  $\gamma_0$  to be the outer connected component of the boundary of  $\Delta_n$ . Let  $s = \text{sgn det } DF(p)$ ,  $p \in \Delta_n$ . Then*

$$r(F(\gamma_0)) = r(F(\gamma_1)) + \dots + r(F(\gamma_n)) - s(n - 1).$$

In particular, if  $n = 1$ , we learn that if  $r(F(\gamma_0)) = r(F(\gamma_1))$ , in agreement with lemma 12.

**Proof:** Construct  $n$  smooth disjoint arcs  $\delta_1, \dots, \delta_n$  such that  $\delta_j$  crosses  $\gamma_0$  and  $\gamma_j$  transversally at points  $p_j$  and  $\tilde{p}_j$ , respectively, as in figure 12 (a). Construct a simple pre-curve  $\gamma$  in the interior of  $\Delta_n - \cup_i \delta_i$  close to its boundary, as indicated in figure 12 (b). From proposition 13,  $r(F(\gamma)) = s$ .

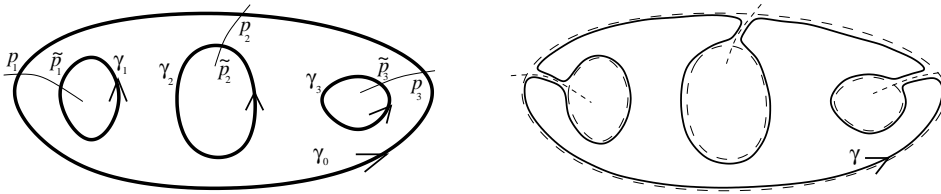


Figure 12: Adding rotation numbers

On the other hand,

$$r(F(\gamma)) = r(F(\gamma_0)) - r(F(\gamma_1)) - \dots - r(F(\gamma_n)) + sn.$$

Indeed, the parts of  $\gamma$  close to some  $\gamma_i$  contribute to  $r(F(\gamma))$ , up to a small error, with  $r(F(\gamma_0)) - r(F(\gamma_1)) - \dots - r(F(\gamma_n))$ . Similarly, the parts of  $\gamma$  near some  $\delta_j$  contribute, again up to a small error, with 0 since arcs on either side of  $\delta_j$  essentially cancel their contributions. For each of the  $2n$  intersections between some  $\gamma_i$  and some  $\delta_j$ , there are two small arcs of  $\gamma$  which together contribute with half a turn, more precisely, with approximately  $s/2$ . Finally, the small errors cancel each other since both right and left hand side are integers. ■

A cusp  $q$  in a closed critical curve  $\Gamma$  is an *inner* (resp. *outer*) cusp if it is effective on the bounded (resp. unbounded) component of  $\mathbb{R}^2 - \Gamma$ .

**Proposition 15** *Let  $F : \mathbb{R}^2 \rightarrow \mathbb{R}^2$  be an excellent smooth function with critical set  $C$ . Let  $A$  be a closed annulus containing a single critical curve  $\Gamma = A \cap C$ ; set  $\gamma_{in}$  and  $\gamma_{out}$  to be the positively oriented simple closed components of the boundary of  $A$ , assumed to be smooth. Let  $k_{in}$  and  $k_{out}$  be the number of inner and outer effective cusps on  $\Gamma$  and let  $s_{in} = \text{sgn det } DF(p_{in})$ ,  $p_{in} \in \gamma_{in}$  and  $s_{out} = -s_{in} = \text{sgn det } DF(p_{out})$ ,  $p_{out} \in \gamma_{out}$ . Then*

$$r(F(\gamma_{out})) = r(F(\gamma_{in})) + s_{in}k_{in} + s_{out}k_{out}.$$

**Proof:** Given proposition 14 (with  $n = 1$ ) we may assume  $\gamma_{in}$  and  $\gamma_{out}$  to be very near  $\Gamma$  and for their tangent vectors to be likewise near the tangent vectors to  $\Gamma$ . We first deform  $\gamma_{in} = \gamma_0$  into  $\gamma_1$ , a curve which coincides with  $\gamma_{out}$  except in small neighborhoods of cusps. If in the process the tangent vectors to intermediate curves  $\gamma_s$ ,  $s \in [0, 1]$ , are kept almost parallel to the tangent vectors to  $\Gamma$ , they will never lie in the kernel of  $DF$  (which, due to the normal form at folds, is never tangent to  $\Gamma$ ) and thus  $F(\gamma_s)$  are all regular and  $r(F(\gamma_1)) = r(F(\gamma_{in}))$ .

Let  $\gamma_2$  be a curve which coincides with  $\gamma_1$  everywhere except in the neighborhood of a cusp  $p_c$ , where  $\gamma_2$  coincides with  $\gamma_{out}$ . We now compare  $r(F(\gamma_2))$  and  $r(F(\gamma_1))$ . The region where  $\gamma_1$  and  $\gamma_2$  do not coincide lies in a small neighborhood of  $p_c$  and we may therefore use the normal form at cusps:  $r(F(\gamma_2)) - r(F(\gamma_1)) = \text{sgn det } DF(p)$ , where  $p$  is in the region where the cusp  $p_c$  is effective. Repeating this process for the other curves yields the desired result. ■

As an application, we perform some tests on  $F_0$ . Suppose that we know that the critical set  $C$  contains (at least) the curves  $\Gamma_1$  and  $\Gamma_2$  as indicated in figure 6. Let  $D_{\Gamma_1}$  and  $D_{\Gamma_2}$  be the topological disks bounded by these curves. Consider four simple, positively oriented closed curves  $\gamma_{in,1}$ ,  $\gamma_{out,1}$ ,  $\gamma_{in,2}$ ,  $\gamma_{out,2}$ , on both sides of the critical curves, as in proposition 15. From the knowledge of the images of these four curves we learn that  $r(F_0(\gamma_{in,1})) = 1$ ,  $r(F_0(\gamma_{out,1})) = -2$ ,  $r(F_0(\gamma_{in,2})) = -2$  and  $r(F_0(\gamma_{out,2})) = 3$ . Cusps on  $\Gamma_j$ ,  $j = 1, 2$  are effective on the outside of  $D_{\Gamma_j}$ ; these values are therefore in agreement with proposition 15.

If the rotation number of  $F_0(\gamma_{in,1})$  were different from 1, we would learn from proposition 13 that there had to be additional critical curves in  $D_{\Gamma_1}$ . Similarly, proposition 14 would indicate the presence of critical curves in the annulus

bounded by  $\Gamma_1$  and  $\Gamma_2$  if the rotation numbers  $r(F_0(\gamma_{out,1}))$  and  $r(F_0(\gamma_{in,2}))$  were different. Finally, again by proposition 14,  $r(F_0(\gamma_{out,2})) = 3$  is compatible with the behavior of  $F_0$  at infinity.

Given a nice function  $F$  and a subset  $C_1$  of the critical set  $C$ , our criteria never guarantee that  $C_1 = C$ . There is a more complicated theorem which provides necessary and sufficient conditions for the existence of a nice function  $F_1$  coinciding with  $F$  in a neighborhood of  $C_1$  and having  $C_1$  as critical set. Theorem 3.1 in [13] (or theorem 1.6 in [14] for the simpler case of bounded critical sets) makes use of the ingredients used in this text, combined with an additional tool from combinatorial topology—Blank-Troyer theory ([18], [21]). Whether  $C_1$  is the critical set of  $F$  is something that cannot be resolved without invoking completely different methods. The difficulty is already evident in one dimension: how do you know that your favorite numerical method has found all the roots of, say, the real function  $f(x) = x^7$ ? If one is only entitled to a finite number of evaluations of a function and its derivatives, one will never know what happens on very small scales or at very remote points.

## 10 Other examples

Consider the variation on  $F_0$  given by  $F_1(z) = z^7 + \bar{z}^4 + z$ . Now, the  $\bar{z}^4$  term never dominates, and there is no distinctive intermediate behavior. The critical set, shown in figure 13, consists of six curves, and from their images it is clear that each has three outer cusps. Most points in the image have 7 preimages and the number of preimages of any point ranges from 7 to 11. For the program, both functions are in a sense equally easy to handle.

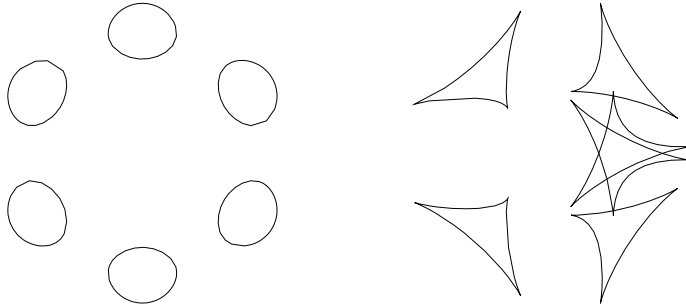


Figure 13: Critical curves of  $F_1$  and their images

Notice that if one of the critical curves had somehow escaped detection then the identity from proposition 14 would have indicated that something was missing. More explicitly, we would consider  $\Delta_5$ , a disk with 5 holes:  $\gamma_0$  would be a large positively oriented circle and  $r(F(\gamma_0)) = 7$  (the degree of  $F_1$ ). On the

other hand,  $\gamma_i$  for  $i = 1, \dots, 5$  would be smooth closed curves just outside known critical curves; from proposition 15,  $r(F(\gamma_i)) = 2$ . Here  $s = 1$  ( $\det DF(p) > 0$  for large  $p$ ) and  $n = 5$ ; proposition 14 would give  $7 = 2 + 2 + 2 + 2 + 2 - 4 = 6$ ; the fact that this is wrong indicates that at least one critical curve is missing.

The *lip* is a simpler example:  $F_2(x, y) = (x, y^3/3 + (x^2 - 1)y)$ , with critical set  $C$  equal to the unit circle and image  $F_2(C)$  given in figure 14. There exists a diffeomorphism  $\tilde{F}_2$  on the plane which coincides with  $F_2$  outside a certain circle around the origin. Thus, the propositions in section 9 would not help us detect topological lips.

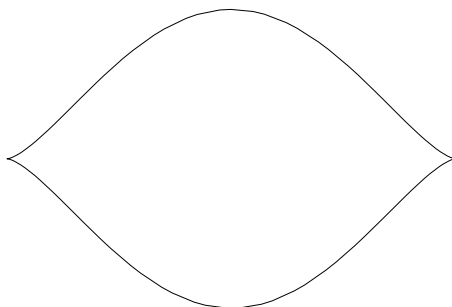


Figure 14: The lip

Our final example is the function  $F_3(x, y) = (x^2 - y^2 + 20 \sin x, 2xy + 20 \cos y)$ . Both  $C$  and  $F(C)$  are given in figure 15; the critical set has 17 components and lips abound. Points in the unbounded tile for  $F(C)$  have two preimages; the origin has 10 preimages.

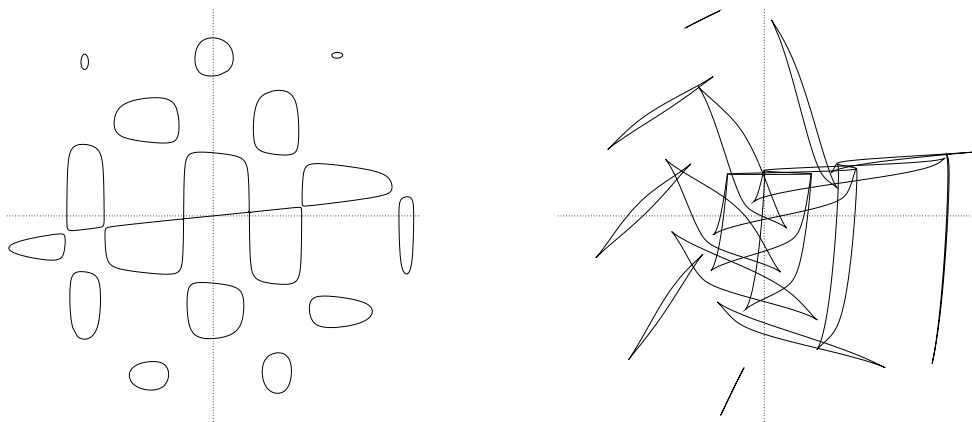


Figure 15: A periodic perturbation of  $z \mapsto z^2$

## Acknowledgements:

This work was supported by CNPq and Faperj (Brazil).

## Address:

Departamento de Matemática, PUC-Rio,  
R. Marquês de S. Vicente 225, Rio de Janeiro, RJ 22453-900, Brazil,  
nicolau@mat.puc-rio.br, tomei@mat.puc-rio.br

## References

- [1] <http://www.mat.puc-rio.br/~nicolau/2x2/2x2.html>.
- [2] Ahlfors, L. V., Complex Analysis, McGraw Hill, London, 1981.
- [3] Allgower, E. L. and Georg, K., Numerical continuation methods: an introduction, Springer-Verlag, New York, 1991.
- [4] Bak, J. and Newman, D. J., Complex analysis, UTM, Springer-Verlag, New York, 1982.
- [5] Chinn, W. G. and Steenrod, N. E., First concepts of topology, New Mathematical Library, MAA, 1966.
- [6] Duczmal, L., Geometria e inversão numérica de funções de uma região limitada do plano no plano, Ph. D. Thesis, PUC-Rio, Rio de Janeiro, 1997.
- [7] Francis, G. K. and Troyer, S. F., Excellent maps with given folds and cusps, Houston J. of Math. 3 (1977), 165–192.
- [8] Golubitsky, M. and Guillemin, V., Stable mappings and their singularities, Graduate Texts in Mathematics 14, Springer-Verlag, New York, 1973.
- [9] Golubitsky, M. and Schaeffer, D., Singularities and groups in bifurcation theory, vol. 1, Applied Mathematical Sciences, 51, Springer-Verlag, New York, 1985.
- [10] Hopf, H., Über die Drehung der Tangenten und Sehnen ebener Kurven, Compositio Math. 2 (1935), 50–62.
- [11] Lang, S., Analysis I, Addison-Wesley, Reading, MA, 1968.
- [12] Lehto, O., Univalent Functions and Teichmüller Spaces, GTM 109, Springer-Verlag, New York, 1987.
- [13] Malta, I., Saldanha, N. C. and Tomei, C., Critical Sets of Proper Whitney Functions in the Plane, Matemática Contemporânea, SBM, vol. 13 (10th Brazilian Topology Meeting), 181–228 (1997).

- [14] Malta, I., Saldanha, N. C. and Tomei, C., The numerical inversion of functions from the plane to the plane, *Mathematics of Computation* 65, no. 216, 1531–1552 (1996).
- [15] Massey, W. S., *A basic course in algebraic topology*, Graduate Texts in Mathematics 127, Springer-Verlag, New York, 1991.
- [16] Munkres, J. R., *Topology: a first course*, Prentice-Hall, Inc., Englewood Cliffs, NJ, 1975.
- [17] Ortega, J. M. and Rheinboldt, W. C., *Iterative solution of nonlinear equation in several variables*, Academic Press, New York, 1970.
- [18] Poénaru, V., Extending immersions of the circle (d’après Samuel Blank), Exposé 342, Séminaire Bourbaki 1967-68, Benjamin, NY, 1969.
- [19] Rudin, W., *Real and Complex Analysis*, Third edition, McGraw-Hill, New York, 1987.
- [20] Thomassen, C., The Jordan-Schönflies theorem and the classification of surfaces *Amer. Math. Monthly*, 99 , 2, 116–130 (1992).
- [21] Troyer, S. F., Extending a boundary immersion to the disk with  $n$  holes, Ph. D. Thesis, Northeastern U., Boston, MA, 1973.
- [22] Whitney, H., On regular closed curves in the plane, *Compositio Math.* 4 (1937), 276–284.
- [23] Whitney, H., On singularities of mappings of Euclidean spaces, I: mappings of the plane into the plane, *Ann. of Math.* 62 (1955), 374–410.